ELSEVIER

TiO$_2$-coated Ni powder as a new cathode material for molten carbonate fuel cells

Ming Zi Hong [a,1], Hyun Suk Lee [b], Min Hyuk Kim [b],
Eun Joo Park [b], Hyung Wook Ha [b], Keon Kim [b,*]

[a] Jilin Institute of Chemical Technology, Jilin 132022, China
[b] Division of Chemistry and Molecular Engineering, Korea University, Seoul 136-701, Korea

Abstract

The properties of a new cathode material of nano-sized TiO$_2$-coated Ni powder for application in molten carbonate fuel cells (MCFCs) are investigated. The material is prepared by a sol–gel method. X-ray diffraction (XRD), field emission-scanning electron microscopy (FE-SEM) with energy dispersive X-ray analysis (EDAX), transmission electron microscopy (TEM) and Raman spectroscopy are employed to characterize the cathode material. The nano-sized TiO$_2$ particles are homogenously coated on the surface of the Ni powder. A stable LiTi$_{1-x}$Ni$_x$O$_2$ phase is formed on the surface of the Ni powder during immersion in molten carbonate at 650 °C. The solubility of the TiO$_2$-coated Ni cathode is about 50% lower compare with that of a pure Ni cathode.

1. Introduction

The molten carbonate fuel cell (MCFC) is expected to provide a highly efficient and environmentally clean means of power generation [1,2]. To be commercially viable, the MCFC should show stable performance for over 40,000 h [3]. There are several problems in achieving this target, one of which is slow dissolution of the state-of-the-art cathode material, NiO, into the electrolyte [4]. This leads to precipitation of nickel into the matrix on the anode side under the prevailing reducing conditions that, in turn causes the formation of a short-circuit in the cell. In addition, dissolution of NiO may coarsen the cathode structure and thereby give rise to deterioration of cathode performance [5,6]. Two different

methods have been adopted to solve this problem. One is to use an alternative electrolyte. More basic molten carbonate using Li/Na eutectic carbonates instead of Li/K eutectic carbonates [7,8] or the addition of alkaline earth metal salts based on Mg or Sr [9] have been found to decrease the rate of Ni dissolution in the electrolyte. The other method is to develop an alternative cathode material. Among many investigated materials, LiCoO$_2$ has been considered to be the most promising alternative cathode material because of its higher stability in molten carbonate and slower dissolution rate compared with NiO. Application of LiCoO$_2$ has problems in terms of scale-up of the electrode area and also has a relatively high manufacturing cost. Recently, LiCoO$_2$-coated NiO, La$_{0.8}$Sr$_{0.2}$CoO$_3$-coated NiO, Co-doped Li-NiO and Co$_3$O$_4$-coated Ni [10–16] have been investigated for suitability as MCFC cathode materials.

Titanium is very resistant to corrosion due to the formation of a passive titanium oxide layer at high temperature. This coating can be used to protect different metals and hence to decrease their corrosion rates [17]. Titanium species

---

* Corresponding author. Tel.: +82 2 3290 3128; fax: +82 2 953 1172.
  E-mail address: kkim@korea.ac.kr (K. Kim).
[1] Present address: 575, Shin-dong, Yeongtong-gu, Suwon-si, Gyeonggi-do, 443-391, Korea Energy Lab. Corporate R&D Center, Samsung SDI Co. Ltd.

have been studied under MCFC operating conditions by several investigators [18–21]. Thermodynamic predictions of the stability have been established for both anodic conditions ($H_2/CO_2/H_2O/CO$) and cathodic conditions (O_2/CO_2) [19,20]. Li_2TiO_3 is known to be the only stable phase in both Li/K and Li/Na eutectic carbonate melts. The electrochemical behaviour of the Ni–Ti alloys has been investigated [18] in molten Li/Na eutectic carbonates at 650 °C under the usual MCFC cathodic conditions. In view of these studies, titanium, titanium oxide, and Ni–Ti alloys are candidate materials for MCFCs.

In this study, we have prepared a new alternative cathode material, viz., TiO_2-coated Ni powder, using a polymeric precursor and a sol–gel method. With this method, scale-up of the cathode by powder coating can be easily achieved. The phase changes of TiO_2-coated Ni powder have been investigated through in situ oxidation in $(Li_{0.62}K_{0.38})_2CO_3$. The stability performance of the prepared cathode in molten carbonate has been assessed by means of solubility measurements.

2. Experimental

2.1. Material synthesis

The TiO_2-coated Ni powder was prepared by a sol–gel method via the procedure shown in Fig. 1. A stoichiometric amount of titanium coating solution (an acidic solution of $(NH_4)_2TiO(C_2O_4)_2 \cdot H_2O$, Aldrich Chem., USA, purity of 99.9+%) was dissolved in water with citric acid (Aldrich Chem., USA, purity of 99.5+%) and ethylene glycol. The citric acid was used as a chelating agent to prevent segregation of the titanium species. After that, Ni powder (filamentary nickel type 255, Inco, USA) was immersed in the solution. The molar ratio of citric acid to ethylene glycol to total metal ions in the solution was 2:1:1. The resultant solution was heated and stirred at 80 °C until a gel precursor was produced. After about 1 h, when water was eliminated, the polymeric
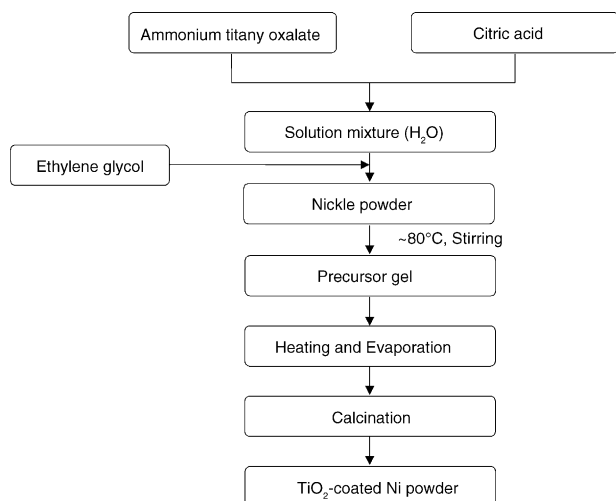

Fig. 1. Procedure for preparing TiO_2-coated Ni powder.

gel was calcined at 500 °C for 3 h in a crucible to remove organic substrate and all decomposable materials.

2.2. Immersion tests

In order to observe phase changes through in situ oxidation of the TiO_2-coated Ni powder in $(Li_{0.62}K_{0.38})_2CO_3$, a 2 g sample of TiO_2-coated Ni powder and 25 g of $(Li:K)_2CO_3$ (62:38 mol%) were placed in an alumina crucible and heated at 650 °C under an air atmosphere for 48 h. The carbonate on the lithiated powder was cleaned with acetic acid, then washed with distilled water, and finally dried in an oven.

The Li content of the TiO_2-coated Ni powder, after immersion treatment in the molten carbonate, was analyzed by atomic absorption spectroscopy (AAS). The sample powder was prepared with various molar ratios of TiO_2:Ni = 0:1.0, 0.1:0.9, 0.2:0.8, 0.5:0.5, 1.0:0. A 0.1 g sample of lithiated TiO_2-coated Ni powder was dissolved in nitric acid (1 M, 5 mL) for 24 h to obtain an analytical solution for AAS.

2.3. Tape-casting and sintering

The TiO_2-coated Ni cathode was made by means of the usual tape-casting method. A binder (2.5 g, MC1500, Hanawa Co., Japan), a plasticizer (1.38 g, glycerol, Junsei Co., Japan) and a defoamer (0.3 g, SN1540, San Nopco Ltd., Korea) were added to the solvent (25 g, toluene:ethanol = 3:7) and subjected to ball milling for 24 h. Then, TiO_2-coated Ni powder (30 g) and dispersant (0.3 g, Cerasperse 5468, San Nopco Ltd., Korea) were added and ball-milled for 5 h. The resulting slurry was completely degassed using a ROTOVAP® evaporator. The TiO_2-coated Ni sheet was dried slowly at room temperature for 24 h. After drying, it was subjected to heat treatment (at a rate of 3 °C per min) under a reducing atmosphere ($H_2:N_2 = 30:70$%) at 750 °C for 30 min.

2.4. Solubility tests

A 2 g sample of the TiO_2 (2.5, 5.0 mol%)-coated Ni cathode and a pure Ni cathode were immersed in 100 g $(Li_{0.62}K_{0.38})_2CO_3$ under at $CO_2:O_2$ (67:33%) atmosphere at 650 °C for 250 h. The equilibrium solubility was determined by removing a ~0.3 g aliquot of the molten carbonate from the melts at the appointed time with an alumina pipette. Each liquid carbonate sample was transferred to a clean alumina crucible, where it was solidified. The melt was purified by a method reported previously [22] and the same design of experimental apparatus for NiO solubility measurement was used. The molten carbonate sample was dissolved in nitric acid (1 M). The content of Ni dissolved into the carbonate melt was determined by AAS.

2.5. Instrumentation

The thermal behaviour of the precursor solution was investigated by thermogravimetric and differential scanning

calorimetry (TGA/DSC, SDT2960). The crystal structures of the as-synthesized powders were determined by X-ray diffraction (XRD, Rigaku Geigerflex DMAX-IIA) with radiation of Cu Kα and at a scan speed of $0.04°s^{-1}$ over a 2θ range of 15–80°, as well as by Raman spectrometry (Jasco, NR-1100, Coherent Innova 70 series Ar ion laser). The morphology and size of the synthesized powders were observed with a field emission scanning electron microscopy (FE-SEM, Hitachi 6300) with energy dispersive X-ray analysis (EDAX) and with a transmission electron microscope (TEM, Philips CM30). The Li content of the lithiated TiO_2-coated Ni powder and the content of Ni dissolved in the carbonate melt were measured by AAS. Porosimetry (Micromeritic 9220) was used to measure the pore-size distribution of the cathodes. A standard test method based on Archimedes' principle (ASTM, C378-88) was used to determine the porosity of the cathodes.

Fig. 3. XRD pattern for TiO_2-coated Ni powder obtained after calcination of gel precursors at 500 °C for 3 h.

3. Results and discussion

3.1. Preparation of TiO_2-coated Ni powder

In order to evaluate the thermal behaviour of the gel precursor, a TGA-DSC technique was employed. The TGA and DSC data for the gel precursors are shown in Fig. 2. In the TGA curve, there are three discrete weight-loss steps between 20 and 250 °C, 250 and 360 °C, and 360 and 500 °C. The first sharp loss in mass is mainly caused by the removal of water and ethylene glycol in the gel precursor and dehydration of the citric acid $-CH_2-CHOH-$ units to $-CH\equiv CH-$. The second mass loss (250–360 °C) is attributed mainly to the decomposition of the citric acid. The final mass loss (360–500 °C) is mainly associated with the decomposition of ammonium oxalate. The DSC curve for the gel precursor confirmed the results of the TGA analysis. The endothermic peaks at 20–250 °C are due to removal of water, and ethylene
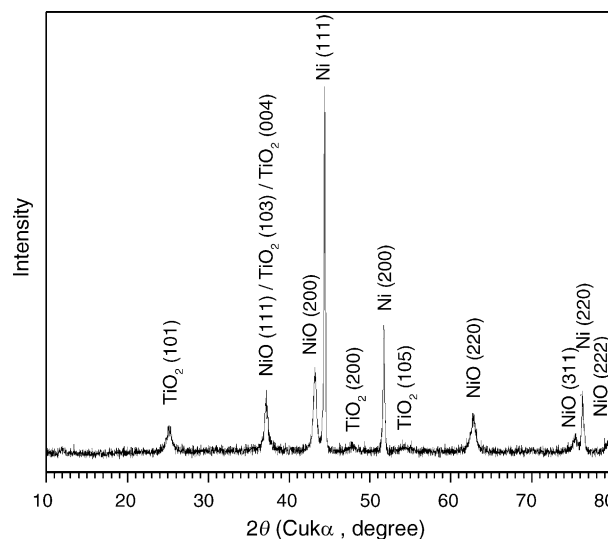
glycol, and to dehydration of the citric acid units [15]. The exothermic peaks at 340–390 °C and 400–500 °C are associated with the decomposition of citric acid and ammonium oxalate, respectively. According to the TGA and DSC curves, the calcination temperature of the gel precursors should be 500 °C, at least. An XRD pattern of the TiO_2-coated Ni powder obtained after calcination of the gel precursor at 500 °C for 3 h is presented in Fig. 3. The XRD pattern contains the major peaks of TiO_2 (JCPDS, File no. 21-1272), Ni (JCPDS, File no. 04-0850), and NiO (JCPDS, File no. 04-0835). The Ti(IV) is known to transform easily into TiO_2 during calcination at 500 °C. Because of this, Ti particles are coated on the surface of the Ni powder so that it reacts easily with oxygen over a large surface area during heat treatment in air. The Ni powder is oxidized during calcination at 500 °C and almost no Ni remains in the metal form [23]. From lattice parameter
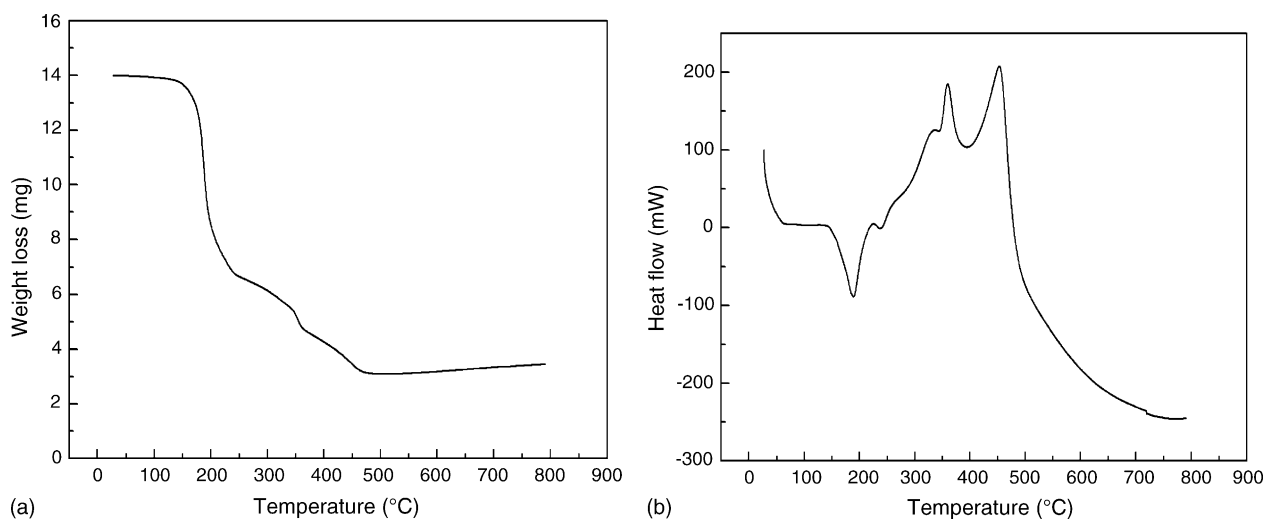

Fig. 2. TGA and DSC curves for gel precursors for TiO_2-coated Ni powder: (a) TGA of gel precursors, (b) DSC of gel precursors.

analysis, it is confirmed that the TiO_2 has not formed a solid solution with the Ni after calcination at 500 °C.

The crystalline size can be calculated from the XRD pattern. A sharp, intense peak corresponds to large particles while broad, weak peaks correspond to small particles. The TiO_2 diffraction peaks (JCPDS, File no. 21-1272) were used to determine the crystallite size by means of the Scherrer equation [Eq. (1)] [24]:

$$L = \frac{0.94\lambda}{B(2\theta)\cos\theta} \tag{1}$$

where λ is the wavelength of the radiation (1.54184 Å for Cu Kα radiation), $B(2\theta)$ is the corrected peak width at half-maximum intensity (FWHM), θ is the peak position, and L is the crystallite size in nanometers. The crystallite size of the TiO_2 particles is found to be about 20 nm after calcination at 500 °C. The TEM image and SAD (selected area diffraction) pattern shown Fig. 4 are for synthesized TiO_2 powder from calcination of ammonium titanyl oxalate + citric acid gel at 500 °C for 3 h. The TEM images confirm the TiO_2 particle size that is determined from XRD data. The TEM analysis also reveals that the nano-sized particles have a wide size-distribution below 50 nm, which is a slightly different to the particle size obtained from XRD data. This is attributed to the fact that the Scherrer equation calculates an average particle size. The SAD pattern displays clear rings, which means that the synthesized powder is very finely crystalline. Scan-
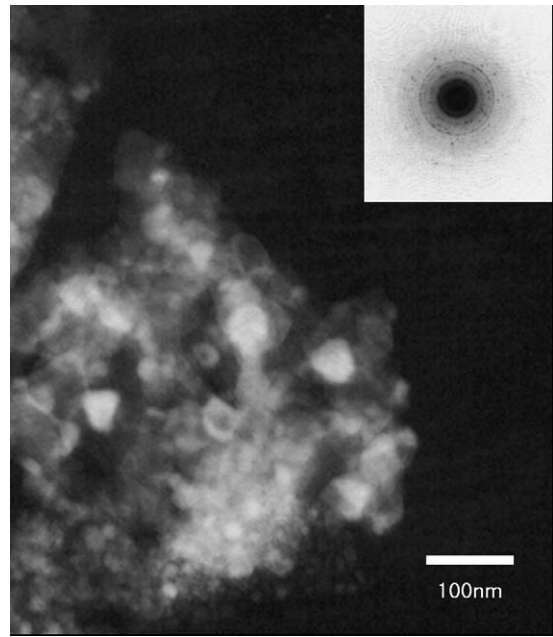

Fig. 4. TEM image and SAD (selected area diffraction) pattern of TiO_2 obtained from calcined ammonium titanyl oxalate + citric acid gel at 500 °C for 3 h.

ning electron micrographs of TiO_2-coated Ni powder and Ti are given in Fig. 5 together with Ni mapping images at the same position. The nano-sized TiO_2 particles do not cause a significant change in the Ni particle size (6–12 μm), which
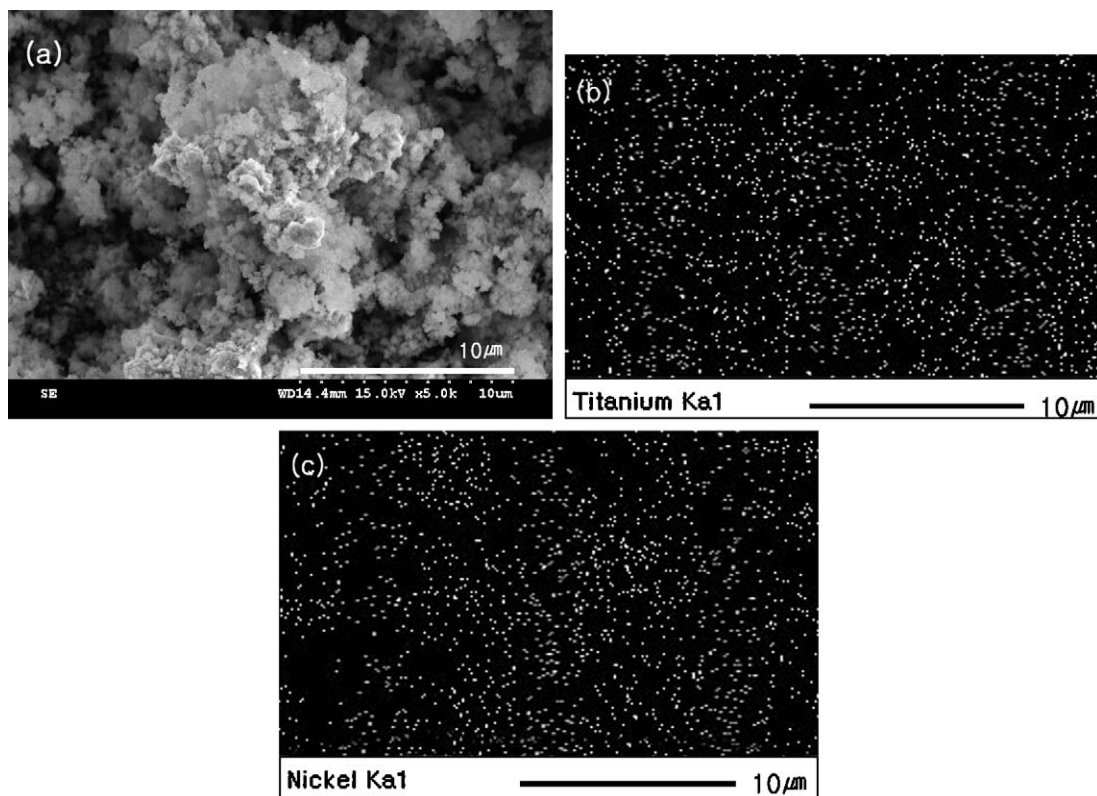

Fig. 5. SEM images of (a) TiO_2-coated Ni powder, (b) Ti mapping, and (c) Ni mapping obtained after calcination at 500 °C for 3 h.
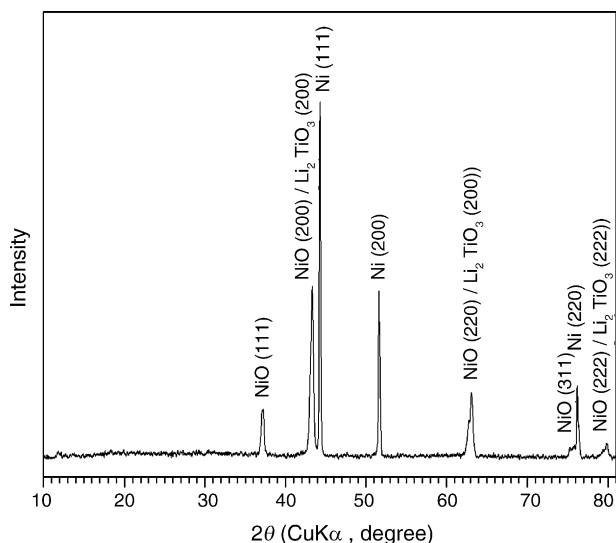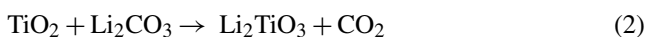
Fig. 6. XRD pattern of TiO_2-coated Ni powder obtained after immersion in molten carbonate at 650 °C for 48 h.

Fig. 7. Li content of lithiated TiO_2-coated Ni powder obtained after immersion in molten carbonate at 650 °C for 48 h.

was well dispersed on the surface of the Ni powder. Both the distributions of Ti and Ni are uniform in the mapping area in Fig. 5(b) and (c). Considering the above results in Figs. 3–5, it can be confirmed that the nano-sized TiO_2 particles are homogeneously coated on the surface of the Ni powder.

3.2. Characterization of TiO_2-coated Ni powder in molten carbonate

TiO_2 is easy to lithiate in the molten carbonate at 650 °C through a reaction as follows [19]:

$$TiO_2 + Li_2CO_3 \rightarrow Li_2TiO_3 + CO_2 \tag{2}$$

Li_2TiO_3 is stable phase in molten carbonate. On the other hand, NiO cannot be easily lithiated in molten carbonate at 650 °C.

The XRD pattern of TiO_2-coated Ni powder obtained after immersion in the molten carbonate at 650 °C for 48 h is shown in Fig. 6. The XRD pattern shows two different structure types, namely, NiO peaks (JCPDS, File no. 04-0835), and Ni peaks (JCPDS, File no. 04-0850), on the other hand lithiated TiO_2 peaks are absent. It is concluded that the major Li_2TiO_3 peaks (JCPDS, File no. 03-1024) that should have appeared at $2\theta = 43.69$, 63.2 and 79.87° are overlapped by NiO peaks. Thus, the lithiated TiO_2 is reconfirmed by AAS. The Li content of each lithiated TiO_2-coated Ni powder prepared with various TiO_2:Ni ratios is shown in Fig. 7, which were measured after immersion in molten carbonate at 650 °C for 48 h. The Li content increases as the TiO_2:Ni ratio is increased. From this fact, it can be concluded that the Li content after immersion in the molten carbonate is mainly due to the lithation of TiO_2 particles on the surface of the Ni powder.

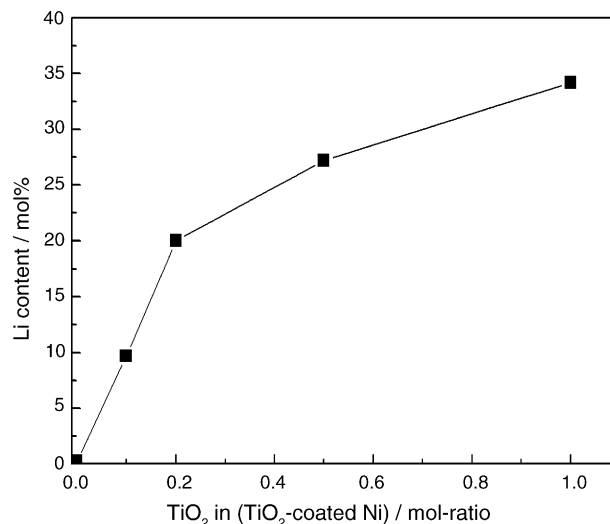Raman spectroscopy was used to observe the phase change of the TiO_2-coated Ni powder in molten carbonate. The

Raman spectra of TiO_2-coated Ni powder obtained after immersion in molten carbonate at 650 °C for 48 h is presented in Fig. 8. Porotnikov et al. [25,26] have interpreted the vibration spectra of Li_2TiO_3 using the results of group theoretical analyses. For lithium titanate, the peaks in the 550–700 cm^{-1} region are known to be due to Ti–O stretching in TiO_6 octahedral. In oxides where lithium has both octahedral and tetrahedral coordination, the Li–O stretching is known to lie within the 250–500 cm^{-1} region. In the Li_2TiO_3 structure, the lithium occupies both octahedral and tetrahedral positions. Further, with increasing TiO_2 coating, the intensities of the peaks decrease and become broader, and the area of the peak increases [27,28]. The increase in area is probably due to cation mixing in the crystal layers as indicated by the incorporation of Ni into Ti sites. The above Raman results suggest that the TiO_2 reacts with Li in molten carbonate to
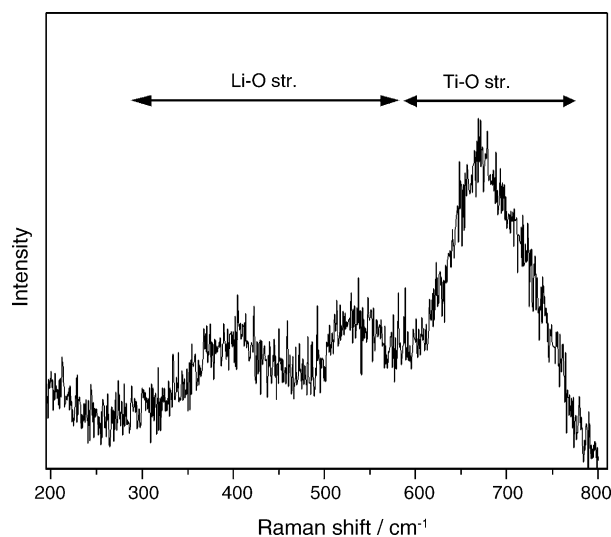

Fig. 8. Raman spectrum of TiO_2-coated Ni powder obtained after immersion in molten carbonate at 650 °C for 48 h.
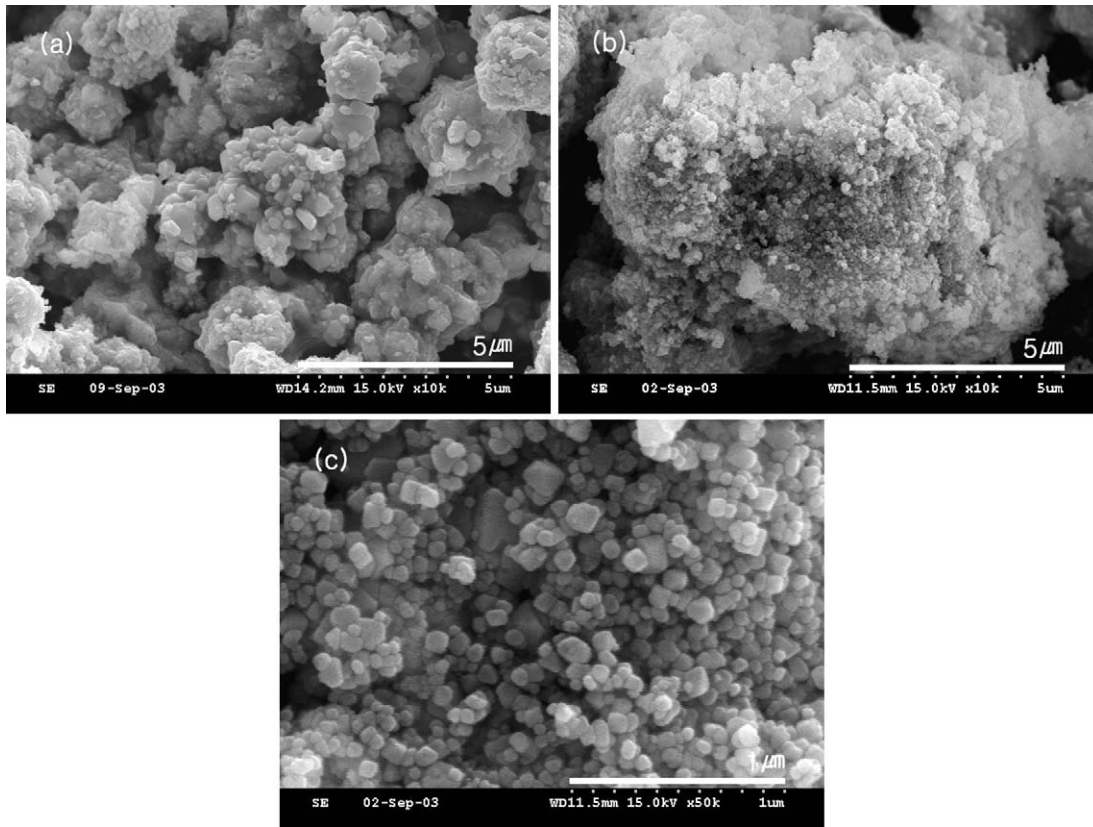
Fig. 9. SEM images of (a) pure Ni powder and (b), (c) TiO$_2$-coated Ni powder obtained after immersion in molten carbonate at 650 °C for 48 h.

form Li$_2$TiO$_3$ during immersion in molten carbonate. As the immersion time increases, the Li$_2$TiO$_3$ phase changes to form a lithiated Ti–Ni solid solution oxide (LiTi$_{1-x}$Ni$_x$O$_2$) in the molten carbonate. Scanning electron micrographs of (a) pure Ni powder and (b), (c) TiO$_2$-coated Ni powder obtained after immersion in molten carbonate at 650 °C for 48 h are given in Fig. 9. In general, the TiO$_2$-coated sample retains the net-

work structure of primary NiO powder and the surface is covered with many tiny grains, see Fig. 9(b). These grains have a complex morphology and are about 100 nm in length, see Fig. 9(c). It is assumed that the grains are composed of Li$_2$TiO$_3$. Lithium could not be detected in the EDAX mapping image of lithiated TiO$_2$-coated Ni powder. On the other hand, the distribution of Ti on the surface of the Ni is relatively
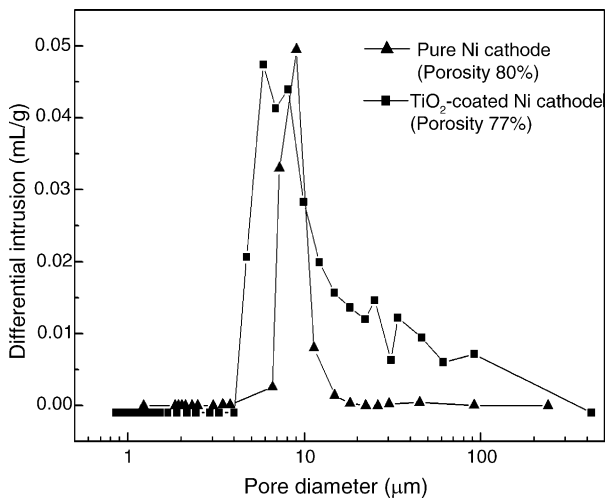

Fig. 10. Pore-size distribution curves for pure Ni cathode and TiO$_2$-coated Ni cathode.
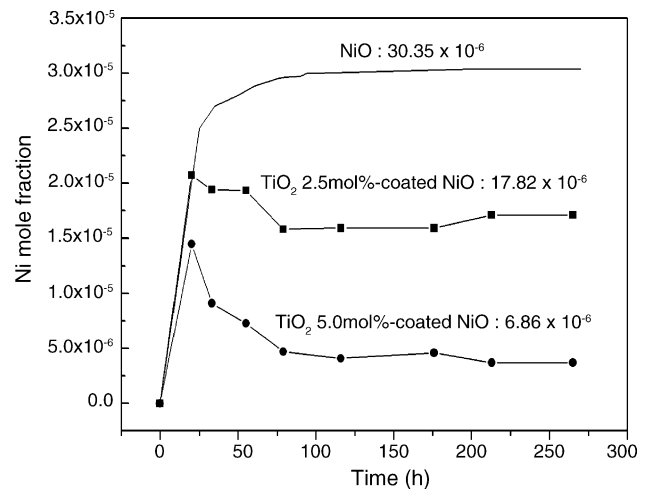

Fig. 11. Solubility of the pure Ni cathode and TiO$_2$ ((■)2.5, (●)5.0 mol%)-coated Ni cathode in (Li$_{0.62}$K$_{0.38}$)$_2$CO$_3$ at 650 °C under CO$_2$:O$_2$ (67:33%).
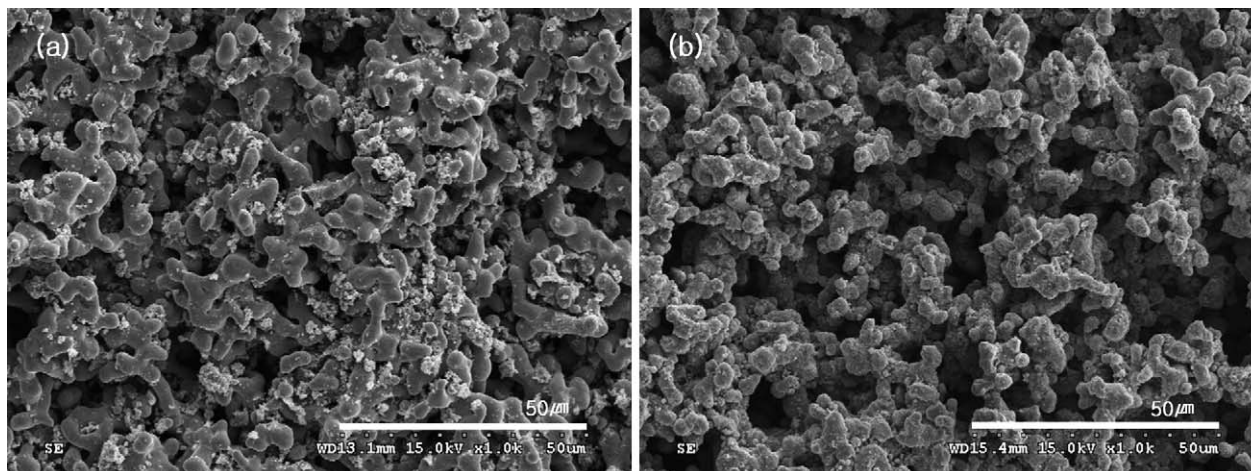
Fig. 12. SEM images of TiO$_2$-coated Ni cathode (a) before and (b) after solubility test at 650°C under CO$_2$:O$_2$ (67:33%).

uniform due to the formation of a stable Li$_2$TiO$_3$ (100 nm) phase on the surface of the NiO powder during immersion in molten carbonate at 650 °C.

3.3. Characterization of TiO$_2$-coated Ni cathode

The pore-size distribution and the porosity of the electrodes are principal determinants of MCFC performance. For example, a very small pore-size distribution and low porosity of the cathode leads to flooding by electrolyte and decreases the cell performance. Therefore, the cathode should have an appropriate average pore size (5–10 μm) and proper porosity (60–80%).

The pore-size distribution of a pure Ni cathode and a TiO$_2$-coated Ni cathode are shown in Fig. 10. The pure Ni and the TiO$_2$-coated Ni cathodes were obtained by sintering of the green sheet made by the tape-casting method at 750 for 30 min in a reducing atmosphere (H$_2$:N$_2$ = 30:70%). The average pore-size and porosity of the TiO$_2$ -coated Ni cathode are about 7 μm and 77%, respectively, which are close to those of the pure Ni cathode, viz., average pore-size about 8 μm and porosity 80%. These findings suggest that the coated nano-sized TiO$_2$ particles do not cause a significant change in the size of the primary Ni particles. Therefore, the physical properties of the prepared cathode are suitable for MCFC.

3.4. Solubility tests

Solubility tests of the cathode in molten carbonate were performed using a pot cell for 250 h, and then the amount of Ni dissolved into the carbonate melt was analyzed by AAS. The results for a pure Ni cathode and TiO$_2$ (2.5, 5.0 mol%)-coated Ni cathodes in (Li$_{0.62}$K$_{0.38}$)$_2$CO$_3$ at 650 °C under a CO$_2$:O$_2$ (67:33%) atmosphere are presented in Fig. 11. The mole fractions of Ni in the carbonate melt increase with time and reach a constant value after about 75 h. The solubility of the NiO cathode is about 30.35 × 10^{-6} mole fractions, which

is similar to the value reported in the literature [29]. On the other hand, the solubility of the TiO$_2$ (2.5, 5.0 mol%)-coated Ni cathodes are about 17.82 × 10^{-6} and 6.86 × 10^{-6} mole fractions, respectively. As shown by the data, the solubility of Ni in mole fractions from TiO$_2$-coated Ni cathodes decreases by about 48 and 77% as the TiO$_2$ content is increased from 2.5 to 5.0 mol%, when compare with that of a pure Ni cathode. The results suggest that the remarkable decrease in solubility is because the stable Li$_2$TiO$_3$ and LiTi$_{1-x}$Ni$_x$O$_2$ phase formed on the NiO prevents dissolution of Ni^{2+} ions into the electrolyte during MCFC operation.

Scanning electron micrographs of the TiO$_2$-coated Ni cathode before and after the solubility test are shown in Fig. 12. There is very little change in the network structure, particle size or pore size. These features indicate that the TiO$_2$-coated Ni cathode can be used as a cathode for long-term operation in MCFCs.

4. Conclusions

The properties of a new alternative cathode for MCFCs have been investigated. The following conclusions have been reached.

(1) The sol–gel method has been used to prepare a homogeneous coating of nano-sized TiO$_2$ particles on the surface of Ni powder.
(2) The TiO$_2$-coated Ni powder forms a stable phase of Li$_2$TiO$_3$ on the surface of NiO powder in (Li$_{0.62}$K$_{0.38}$)CO$_3$ at 650 °C under air atmosphere. The Li content in the powder after immersion in molten carbonate is mainly attributable to lithiation of the TiO$_2$ particles on the surface of the Ni powder.
(3) The TiO$_2$-coated Ni cathode has an appropriate pore-size distribution and porosity for use in MCFCs. The solubility of Ni (in mole fractions) from TiO$_2$-coated Ni cathodes decreases by about 48 and 77% for an increase

in TiO_2 content from 2.5 to 5.0 mol% when compared with a pure Ni cathode in $(Li_{0.62}K_{0.38})_2CO_3$ at 650 °C under a CO_2:O_2 (67:33%) atmosphere. As a result, the TiO_2-coated Ni powder can significantly retard the dissolution of NiO in molten carbonate due to the formation of a stable lithiated Ti–Ni solid solution phase on the surface of the NiO.

(4) The TiO_2-coated Ni powder is a promising alternative cathode material for MCFCs. Using the powder coating method and the sol–gel technique, it is expected that a scaled-up cathode could be easily manufactured, and that the cathode would lengthen the lifetime of MCFCs.

(5) Further studies are necessary to optimize the composition and the electrochemical performance of this new cathode material and to confirm the long-term stability of cells employing this cathode.

Acknowledgement

References

[1] J.R. Selman, in: L.J.M.J. Blomen, M.N. Mugerwa (Eds.), Fuel Cell Systems, Plenum Press, New York, 1993.

[2] L. Goirgi, M. Carewska, M. Patriarca, S. Scaccia, E. Simonetti, A.D. Bartolomeo, J. Power Sources 49 (1994) 227.

[3] J.P.P. Huijsmans, G.J. Kraaij, R.C. Makkus, G. Rietveld, E.F. Sitters, H.T.J. Reijers, J. Power Sources 86 (2000) 117.

[4] G.L. Lee, J.R. Selman, L. Pomp, J. Electrochem. Soc. 140 (2) (1993) 390.

[5] C.E. Baumgartner, J. Am. Ceram. Soc. 69 (2) (1986) 162.

[6] S. Freni, F. Barone, M. Puglisi, Int. J. Energy Res. 22 (1998) 17.

[7] A.P. Brown, G.H. Kucera, M.F. Roche, Fuel cell Seminar, The Fuel Cell Seminar Organising Committee, Washington DC, 1992, 125.

[8] M.L. Orfield, D.A. Shores, J. Electrochem. Soc. 135 (7) (1988) 1662.

[9] J.D. Doyon, T. Gilbert, G. Davis, J. Electrochem. Soc. 134 (12) (1987) 3035.

[10] S.G. Kim, S.P. Yoon, J.H. Han, S.W. Nam, T.H. Lim, S.A. Hong, H.C. Lim, J. Power Sources 112 (2002) 109.

[11] S.T. Kuk, Y.S. Song, K. Kim, J. Power Sources 83 (1999) 50.

[12] S.T. Kuk, Y.S. Song, S.I. Suh, K. Kim, J. Mater. Chem. 11 (2001) 630.

[13] P. Ganesan, H. Colon, B. Haran, B.N. Popov, J. Power Sources 115 (2003) 12.

[14] P. Ganesan, H. Colon, B. Haran, R. White, B.N. Popov, J. Power Sources 111 (2002) 109.

[15] H.S. Lee, M.Z. Hong, S.C. Bae, H.C. Lee, E.J. Park, K. Kim, J. Mater. Chem. 13 (2003) 2626.

[16] M.Z. Hong, S.C. Bae, H.S. Lee, H.C. Lee, Y.-M. Kim, K. Kim, Electrochim. Acta (2003) 4213.

[17] P.C. Innocenzi, M. Guglielmi, M. Gobbin, P. Colombo, J. Eur. Ceram. Soc. 10 (1992) 431.

[18] C. Belhomme, E. Gourba, M. Cassir, C. Tessier, J. Electroanal. Chem. 503 (2001) 69.

[19] V. Chauvaut, M. Cassir, Y. Denos, Electrochim. Acat 43 (1998) 1991.

[20] V. Chauvaut, M. Cassir, J. Electroanal. Chem. 474 (1999) 9.

[21] V. Chauvaut, E. Duval, B. Malinowska, M. Cassir, J. Mater. Sci. 34 (1999) 2015.

[22] K. Ota, S. Mitsushima, S. Kato, S. Asano, H. Yoshitake, N. Kamiya, J. Electrochem. Soc. 139 (1992) 667.

[23] E.A. Gulbransen, K.F. Andrew, J. Electrochem. Soc. 101 (3) (1954) 128.

[24] C.J. Doss, R. Zallen, Phys. Rev. B: Condens. Matter. 48 (21) (1993) 15626.

[25] N.V. Porotnikov, N.G. Chaban, K.I. Petrov, Russ. J. Inorg. Chem. 28 (1983) 1402.

[26] L.V. Golubeva, N.V. Porotnikov, O.I. Kondratov, K.I. Petrov, Russ. J. Inorg. Chem. 35 (1990) 1028.

[27] T. Nakazawa, V. Grismanovs, D. Yamaki, Y. Katano, T. Aruga, Nucl. Inst. and Methods in Physics Research B 206 (2003) 166.

[28] Yamaki Daiju, Nakazawa Tetsuya, Tanifuji Takaaki, Aruga Takeo, Jitsukawa Shiro, Hojou Kiichi, J. Nucl. Mater. 329–333 (2004) 1279.

[29] E. Zhecheva, R. Stoyanova, Solid State Ionics 66 (1993) 143.